Reprinted from ENVIRONMENTAL SCIENCE & TECHNOLOGY, Vol. 24, Page 66, January 1990

Concentration and Fate of Airborne Particles in Museums

William W. Nazaroff,† Lynn G. Salmon, and Glen R. Cass*

Environmental Engineering Science, California Institute of Technology, Pasadena, California 91125

■ To investigate the potential soiling hazard to works of art posed by the deposition of airborne particles, time-resolved measurements were made of the size distribution and chemical composition of particles inside and outside of three southern California museums. The measured indoor aerosol characteristics agree well with predictions of a mathematical model of indoor aerosol dynamics based on measured outdoor aerosol characteristics and building parameters. At all three sites, the fraction of particles entering from outdoor air that deposit onto surfaces varies strongly with particle size, ranging from a minimum of 0.1–0.5% for particles having a diameter in the vicinity of 0.15 μm to greater than 90% for particles larger than 20 μm in diameter. Deposition calculations indicate that, at the rates determined for the study days, enough elemental carbon (soot) would accumulate on vertical surfaces in the museums to yield perceptible soiling in as little as 1 year at one site to as long as 10–40 years at the other two sites.

Introduction

Air pollutant exposure may damage objects kept indoors. This hazard is an acute concern among museum curators (*1*). The objects in their charge often are valued entirely for their visual qualities, characteristics that may be particularly susceptibile to air pollution damage. Furthermore, it is desired to preserve these objects for centuries. Even modest rates of deterioration may yield an unacceptable cumulative effect.

Airborne particles constitute a major class of pollutants that are hazardous to works of art. Deposition of particulate matter onto the surface of an object may cause chemical damage and/or soiling. Consequently, activities that generate particles, such as smoking, are restricted in museum galleries. However, regardless of the presence or absence of indoor emissions, particulate matter may enter the building with the outdoor air that is supplied for ventilation. Although some research has been reported on indoor/outdoor relationships for airborne particles (e.g., ref 2 and references therein), little is known about particle concentrations in museums, the factors that affect those concentrations, the fate of particles that enter museum atmospheres, and the magnitude of the soiling hazard posed by deposition of airborne particles (*3*). The present paper addresses these issues.

Over periods of 24 h, at each of three museums in southern California, time-dependent measurements were made of the chemical composition and size distribution of the indoor and outdoor aerosol. Building characteristics that influence aerosol concentrations and fates were measured: ventilation rate, temperature differences between a wall and the air, fluid velocities adjacent to a wall, and the particle removal efficiency of filters in the mechanical ventilation system. From these data, the concentrations and fates of indoor particles were computed for each site, by use of a mathematical model previously developed for this study (*4*). To evaluate model performance, predicted indoor aerosol properties—based on measured outdoor aerosol data and building characteristics—were compared against the results of the indoor measurements. The fate of particulate matter entering the museums was assessed with the model, emphasizing the deposition of particles—particularly those containing elemental carbon and soil dust—onto indoor surfaces. Results indicate that the rate of deposition of elemental carbon (soot) particles onto museum surfaces is sufficient to produce perceptible soiling over time periods that are short relative to the desired lifetimes of works of art. The results also suggest that the principal soiling hazard to smooth vertical surfaces and to downward facing surfaces results from the deposition of particles with diameters in the vicinity of 0.1 μm. For floors and other upward facing surfaces, both fine and coarse particles contribute significantly to the rate of soiling.

Table I. Characteristics of the Study Sites

	Norton Simon	Scott Gallery	Sepulveda House
dimensions			
no. of floors	2	1	2
floor area, m^2	4930	535	330
wall area, m^2	6950	1990	1050
volume, m^3	21540	2530	1200
ventilation[a]			
outdoor air-exchange, h^{-1}	0.37[b]	0.28 ± 0.01	3.6 ± 1.4
recirculation, h^{-1}	5.8	8.2	
monitoring period			
start date	6 April 88[c]	24 April 88	30 March 88
start time	1000 PDT	1800 PDT	2100 PST

[a] Flow rate divided by building volume; mean ± SD of measurements for 24-h period. [b] Based on hot-wire anemometry measurements of outdoor air flow rate into mechanical ventilation system. Tracer gas decay yielded 0.40 h^{-1} with 90% confidence bounds of 0.37–0.44 h^{-1}. [c] Boundary layer flow and temperature differences measured for 24 h commencing at 1200 PDT on 4 April 1988.

Study Sites

Three sites in southern California were selected for the study: the Norton Simon Museum in Pasadena, the Scott Gallery on the Huntington Library grounds in San Marino, and the Sepulveda House at El Pueblo de Los Angeles State Historic Park in downtown Los Angeles. These were chosen from among five museums in which indoor and outdoor aerosol characteristics were measured on a 24-h-average basis every sixth day during the previous summer and winter seasons (*5*). The range of values for the ratio of indoor to outdoor aerosol mass concentration thus was

†Present address: Department of Civil Engineering, University of California, Berkeley, CA 94720.

0013-936X/89/0924-0066$02.50/0

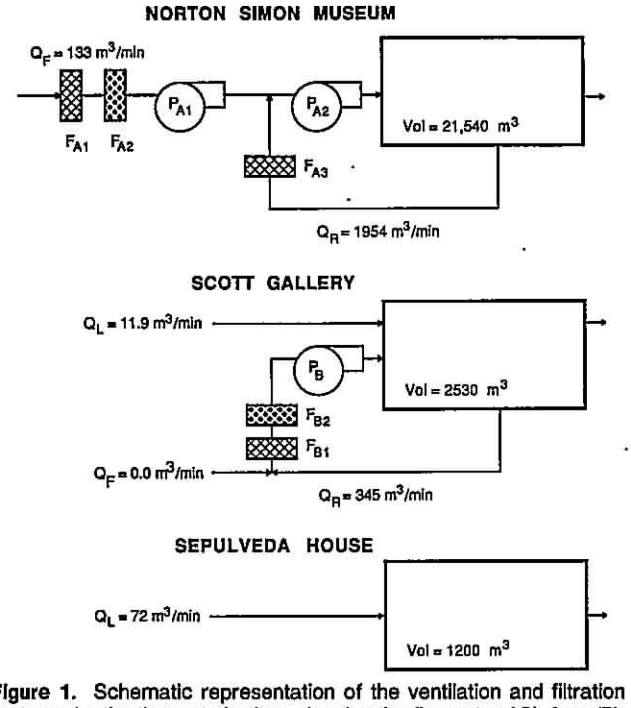

Figure 1. Schematic representation of the ventilation and filtration systems for the three study sites, showing the flow rates (Q), fans (P), and filters (F) in each system. For air flows, subscripts L, F, and R represent leakage (infiltration), forced supply (make-up), and recirculation, respectively. Filters F_{A2} and F_{B2} contain activated carbon for ozone removal; the other filters are mat-fiber type for removing particles.

known in advance, and the three sites were selected to span the range from high to low indoor aerosol concentration. Major characteristics of the buildings are summarized in Table I and in the following discussion.

The Norton Simon Museum and the Scott Gallery are modern buildings with custom-engineered heating, ventilation, and air conditioning (HVAC) systems (see Figure 1). At the Norton Simon Museum, make-up air from outdoors passes through a fibrous mat filter (F_{A1}), and through an activated carbon filter (F_{A2}), before being blended with return air that has been passed through a fibrous mat filter (F_{A3}); the air mixture is then conditioned for proper temperature and humidity and distributed to the building. At the Scott Gallery, the flow rate of make-up air was recently reduced effectively to zero by closing the intake dampers. At the time of the present study, air exchange between indoors and outside occurred entirely due to infiltration through cracks in the building shell and through door openings. Recirculated air is passed through a fibrous mat filter (F_{B1}) and an activated carbon filter that was recently added to the system for ozone removal (cf. ref 6).

The Sepulveda House is an historical museum with no HVAC system. Air exchange is provided by infiltration through relatively large openings in the building shell. When the building is open to the public (1000–1500 daily, except Sunday) and the weather is warm, two downstairs doors are kept open.

At each site, one wall was selected for investigation of boundary-layer air flows and temperature gradients that influence particle deposition rates. Measurements of particle deposition rate, reported elsewhere (*7*, *8*), were made on the same walls. A detailed description of the walls is provided in ref 8. Briefly, an interior wall with a painted dry-wall surface was selected for investigation at the Norton Simon Museum; a painted plywood panel mounted onto an interior wall with furring strips was selected at the Scott Gallery; and an outer brick wall having a painted, irregular plaster surface was chosen at the Sepulveda House.

Because the experiments would have been disruptive to normal museum operation, measurements at the Norton Simon Museum and at the Scott Gallery were conducted while the buildings were closed to the public (museum staff were still present). Consequently, the measurements at these sites do not fully incorporate the effects of occupancy on aerosol properties, including particle generation by occupant activities. The Sepulveda House was open to the public, as usual, from 10 a.m. to 3 p.m. on the day of monitoring.

Experimental Methods

Detailed, time-resolved information on the indoor and outdoor aerosol size distribution and chemical composition was collected at each site for a period of 24 h. To measure the aerosol size distribution, two pairs of optical particle counters were operated, one pair sampling from a central indoor location with the second sampling from an outdoor location on the grounds of the site. One instrument in each pair (Particle Measuring Systems Model ASASP-X, referred to subsequently as the "midrange OPC") is capable of detecting particles over a nominal size range of 0.09–3-μm optical diameter and classifying them, according to the amount of light scattered in the forward direction, into 32 size channels. Sampling flow rates were measured and recorded at least hourly with rotameters that had been calibrated against a bubble flow meter; the flow rate was adjusted whenever it deviated by more than 10% from a nominal rate of 1 $cm^3 s^{-1}$. The second instrument in each pair (Particle Measuring Systems Model CSASP-100HV, referred to as the "large-particle OPC") detects and classifies light scattered from particles in the size range 0.5–47-μm diameter. All of the optical particle counters were operated continuously, with cumulative counts per channel recorded at 6-min intervals.

Several tests were conducted with the OPCs to investigate instrument performance (*9*). The performance of the midrange OPCs was good in all of the tests. However, the large-particle OPCs failed to yield satisfactory results in these tests, and consequently, the data from the large-particle OPCs were not used in the analyses reported in this paper.

Indoor and outdoor aerosol mass concentration and chemical composition were determined for total suspended particulate matter (TSP) and for fine particles ($<\sim$2-μm diameter) by using sampling devices and analysis methods similar to those described by Gray et al. (*10*). Briefly, for indoor and outdoor sampling locations, air was drawn through each of two sets of three 47-mm-diameter filters—one quartz fiber (Pallflex 2500 QAO) and two Teflon membrane filters (Gelman, PTFE, ringed, 2.0-μm pore size). One filter set at each site was deployed in open-faced holders to collect the TSP, while the other set was placed within in-line holders downstream of a cyclone separator (*11*) to collect the fine particles. The air flow rate through each filter holder was nominally 30 L min^{-1}, and each of the fine particle filter holders was preceded by its own cyclone separator. The sampling interval was typically 4 h; however, because of access restrictions, 8-h intervals were used at night at the Norton Simon Museum. The quartz filters were analyzed for elemental and organic carbon (*12*, *13*). One of the Teflon filters was used to gravimetrically determine aerosol mass concentration and, by X-ray fluorescence, the concentrations of 34 trace metals (*14*). The second Teflon filter was analyzed for sulfate and nitrate concentrations by ion chromatography

(*15*) and for ammonium ion by colorimetry (*16*). For the purpose of this paper, the elemental carbon concentrations are of great interest, as this component governs the blackness of fine particulate matter (*17*), and therefore a major portion of the soiling hazard. In addition, the aluminum and silicon concentrations are useful markers for soil dust that may contribute to soiling.

Air-exchange rates were measured at each site by the tracer-gas decay technique, with sulfur hexafluoride as the tracer (*18*). At the Scott Gallery and the Sepulveda House, SF_6 measurements were made continuously throughout the study period, with samples collected at intervals of ~10 min and analyzed with a portable gas chromatograph. At the Norton Simon Museum, because of access restrictions, a single 2-h tracer decay measurement was made during the study period. The air flow rates through the mechanical ventilation system were determined by hot-wire anemometry at the Norton Simon Museum and on the basis of building design specifications at the Scott Gallery.

The air velocity adjacent to surfaces and the temperature difference between the surface and the adjacent air are important factors governing the deposition rate of fine particles (*19,20*). During the study period, continuous measurements were made of the temperature difference between the air and the surface of one wall by using an array of thermistors (Yellow Springs Instrument, part no. 44202). Two thermistors were used to determine the temperature of the wall surface; one was mounted in a thin (1.5-mm) aluminum plate that was attached to the wall with thermal joint compound, the other was coated with thermal joint compound and set into a small hole drilled in the wall so that the thermistor was flush with the surface. Likewise, two thermistors were used to determine the air temperature at approximately 15 cm from the wall; one was shielded with insulating foam to eliminate radiant heat transfer; the other was unshielded. The wall–air temperature difference was determined as the difference between the mean of the two wall probes and the mean of the two air probes. The probes were individually calibrated and have an intrinsic uncertainty of ~0.02 °C. Differences in paired temperature measurements for the two wall probes and for the two air probes were less than 0.1 °C in 53%, less than 0.2 °C in 83%, and less than 0.3 °C in 94% of the measurements made during the entire study.

Air velocity was measured adjacent to the same wall by use of two omnidirectional sensors (TSI Model 1620), placed at approximately 0.6 and 1.2 cm from the surface of the wall. The temperatures and velocities were sampled with a microcomputer-based data logger at intervals of 2 s, and the mean value was recorded for each minute. At the Norton Simon Museum, again because of access limitations, surface and air temperatures and the air velocities were monitored for 24 h 2 days prior to the aerosol monitoring period. At the other sites, the temperatures and velocities were measured simultaneously with aerosol monitoring.

The particle removal efficiency of the filters found in the buildings' mechanical ventilation systems was measured as a function of particle size for each fiber filter by simultaneously measuring the upstream and downstream particle concentrations with the two sets of optical particle counters. The measurements at the Norton Simon Museum were done in situ. For filter F_{B1} at the Scott Gallery, a section of a used filter panel from the site was obtained. At a Caltech laboratory (located ~1.5 km from the Scott Gallery), outdoor air was drawn through the filter section at the same face velocity as for actual use of the filter, and the percent removal as a function of particle size was determined.

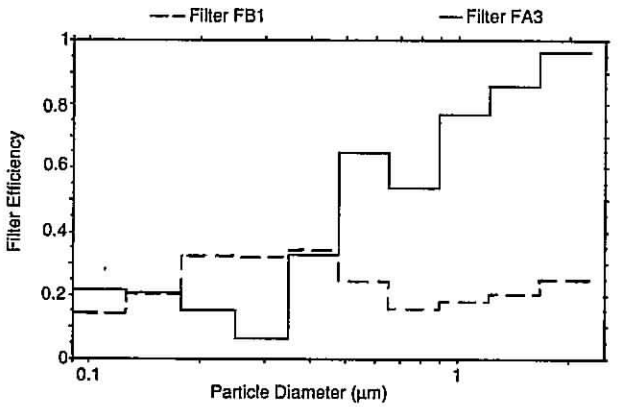

Figure 2. Filtration efficiency of particle filters as a function of particle size. The results are based on 21 and 4.5 h of data for filters F_{A3} and F_{B1}, respectively. The corresponding operating flow velocities across the filter faces are 0.44 and 1.7 m s^{-1}. Filter media: filter F_{A3} is Servodyne type SR-P1L; filter F_{B1} is Servodyne type Mark 80. Filter F_{A1} was found to have less than 5% removal efficiency when new for particles smaller than 2.3 μm in diameter.

Measurement and Modeling Results: Aerosol Size Distribution and Chemical Composition

Filter Efficiency. The filtration efficiency as a function of particle size for a single pass through the building ventilation system filters F_{A3} and F_{B1} is shown in Figure 2. The efficiency for particles in size interval i, η_i, was computed as

$$\eta_i = \frac{C_{u_i} - C_{d_i}}{C_{u_i}} \quad (1)$$

where C_{u_i} and C_{d_i} are the measured upstream and downstream particle volume concentration in size range i, respectively.

At the Norton Simon Museum, filter F_{A1} is composed of the same material as filter F_{A3}. However, whereas filter F_{A3} was sufficiently loaded with particulate matter to appear heavily soiled, new filter material had recently been installed for F_{A1}. Very little difference (<5%) between upstream and downstream particle concentrations was observed for all particle sizes measured for filter F_{A1}. (These observations are consistent with the general knowledge that particle filters become more efficient as the loading increases.) Measurements across the charcoal filter, F_{A2}, indicate that it also is ineffective in removing fine particles.

Temperature Differences and Boundary-Layer Flows. The results of monitoring temperature difference and near-surface air velocity at three sites are shown in Figure 3. The prominent features of the temperature difference profiles are readily understood. For example, the largest peak in $T_{wall} - T_{air}$ at the Norton Simon Museum occurs in the late afternoon. At this time, the air temperature in this gallery increases due to solar heating of the roof and the south and west-facing walls. The mechanical ventilation system supplies cool air in an attempt to maintain the set point temperature, thereby increasing $T_{wall} - T_{air}$ (see also ref 8). (During the long-term monitoring reported in ref 8, a west-facing window opposite the monitored wall was covered by foam board and curtains. Before the present study, the foam board was removed. Consequently, during the afternoon, a portion of the wall was in direct sun, which probably contributed to the peak in $T_{wall} - T_{air}$.) The large dip and rise in the profile at the Scott Gallery is associated with an inad-

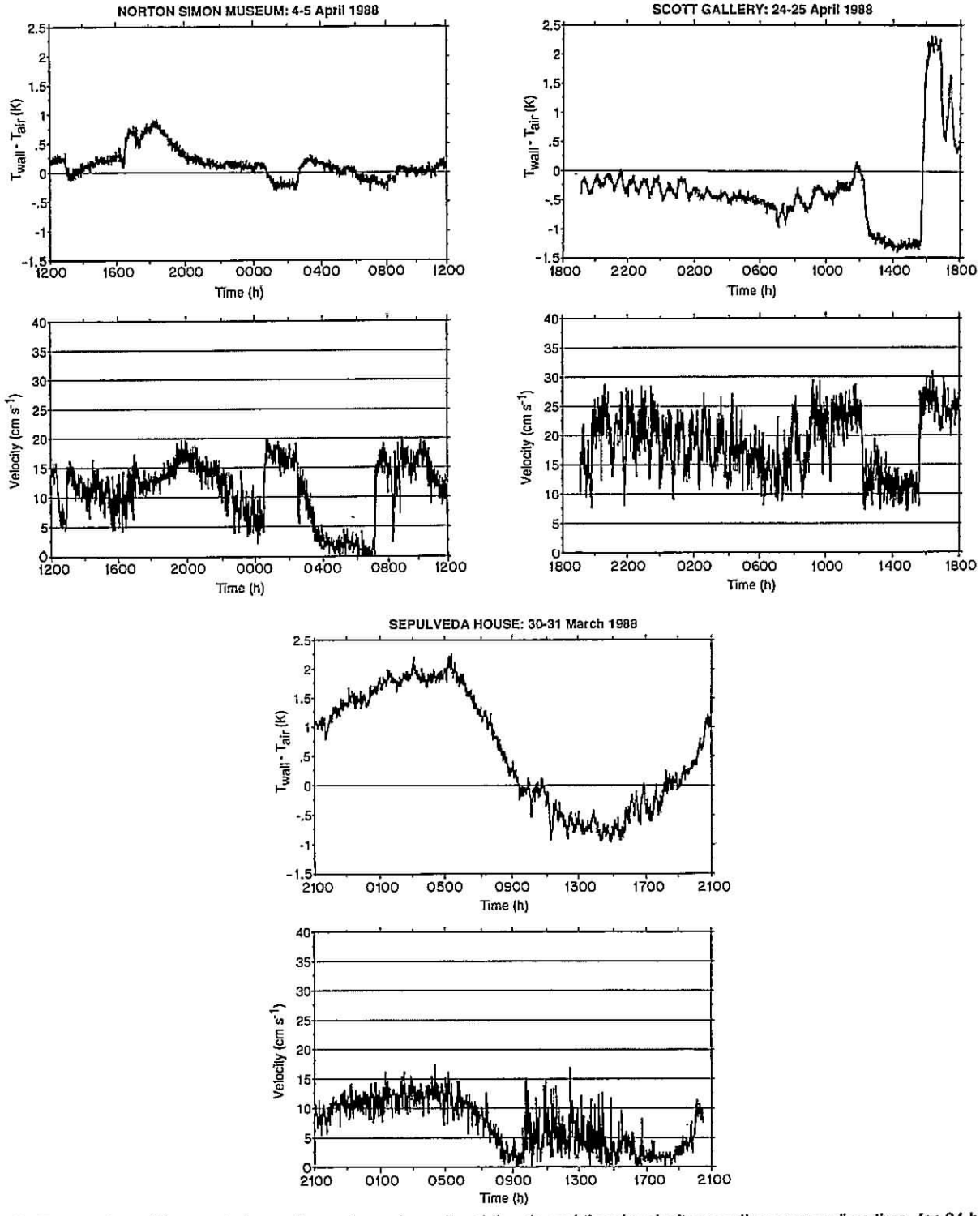

Figure 3. Temperature difference between the surface of a wall and the air, and the air velocity near the same wall vs time, for 24-h periods at each site. The air velocity probe was located at a distance from the wall of 1.05 cm for the Norton Simon Museum, 1.3 cm for the Scott Gallery, and 1.2 cm for the Sepulveda House.

vertent interruption in air conditioning for the building during the period 1200–1545 PDT. (It appears that the fans in the mechanical ventilation system continued to operate during this time, but that the cooling function ceased for almost 4 h.) The indoor air temperature rises rapidly at 1200 PDT and heat is transferred to the (interior) wall. At approximately 1545 PDT, the air-conditioning system resumes operation, rapidly cooling the air, and heat is transferred from the wall back to the air. At the Sepulveda House, without any thermal control, the diurnal cycle is driven by the outdoor air temperature and the delayed thermal response of the brick wall. The maximum value of $T_{wall} - T_{air}$ occurs just before dawn and the minimum occurs at 1400 PST, corresponding approximately to the peak outdoor air temperature.

At the Sepulveda House the near-wall air velocity is consistent with expectations for natural convection (*21,22*), driven by the temperature difference between the wall and the air, for the periods 0000–1000 and 1500–2400 PST, i.e., whenever the museum is closed. Note that during these periods, the maximum velocity occurs when the temperature difference is greatest; likewise, when the temperature difference is near zero, the air velocity is very small. When the museum is open, the air flow velocity adjacent to the

wall is highly variable and appears to be driven predominantly by turbulent air movement in the core of the room.

At the Scott Gallery, the near-wall air velocity appears to be strongly dominated by the flow of air within the building due to the operation of the mechanical ventilation system. At this site, the supply and return-air registers are located at the tops of the walls. The lower velocity observed during the period when air cooling failed probably results from the fact that the buoyant warm air entering the room from the ceiling registers would not promote convective mixing in the core of the room. After cooling is restored, peak near-wall air velocities are observed. A similar correlation between the wall–air temperature difference and the near-wall air velocity is observed at other times during the monitoring period, most notably for the first 7 h. During this interval $T_{wall} - T_{air}$ oscillates with an amplitude of ~0.3 K and a period of approximately 45 min; an envelope of the near-wall air velocity can be traced with an amplitude of approximately 5 cm s^{-1} and the same period. Some of the high-frequency fluctuations in the air velocity at the Scott Gallery may be a result of the fact that the sampling location was located near a door that was opened and closed approximately 10 times hourly during monitoring.

At the Norton Simon Museum, air is supplied to the gallery through perforated tiles that cover more than half of the ceiling. Air is returned to the ventilation system through the interior hallways of the building. Given the combination of this circulation pattern with a lower recirculation rate (see Table I), it is not surprising that the measured near-wall air velocities are generally lower at this site than at the Scott Gallery.

Modeling Aerosol Characteristics. The indoor aerosol size distribution and chemical composition were computed from measured outdoor aerosol properties for each site by use of the indoor air quality model previously reported (*4*). That model tracks the evolution of the indoor aerosol size distribution and chemical composition as it is affected by ventilation, filtration, emission, coagulation, and deposition. For the present study, the aerosol size distribution was represented by 15 sections spanning the diameter range 0.05–40 μm and by three chemical components—elemental carbon, soil dust, and "other".

Measured outdoor concentrations were used as input to the model as follows. Hourly averaged results from the outdoor midrange OPC were used to compute the total mass concentration per section for sections 2–11, assuming the particle density to be 2.0 g cm^{-3} (see ref 9). The total mass concentration for sections 12–15 was determined from filter-based coarse particle concentration measurements, assuming that the mass is distributed uniformly with the log of the particle diameter. Concentrations of elemental carbon and soil dust were determined from analyses of filter samples. The fine elemental carbon concentrations were partitioned into sections 1–11 by using size distribution data reported by Ouimette (*23*) for the Los Angeles and Pasadena elemental carbon aerosol. The concentration of soil dust was computed from the aluminum and silicon content of the aerosol with the data of Miller et al. (*24*) on the percent of these elements in suspended samples of local soil dust. The fine soil dust was apportioned into sections 2–11 in proportion to the size distribution of the total 24-h-average aerosol mass in these sections. For coarse particles both elemental carbon and soil dust were allocated to produce a constant value of $dM/d(\log d_p)$ across sections 12–15, where M is the aerosol mass concentration and d_p is the particle diameter. For section 1, spanning particle diameters in the range of 0.05–0.09 μm, the total aerosol mass of material other than elemental carbon is unknown, and for this paper that other material is neglected. For sections 2–15, the component "other" was determined by difference between the total aerosol mass and the soil dust plus elemental carbon mass.

Table II. Deposition and Filtration Conditions Simulated at Study Sites by Using the Indoor Air Quality Model

case	conditions
	Norton Simon Museum
A	deposition: forced laminar flow; filter F_{A1}: ineffective
B	deposition: homogeneous turbulence in the core of the room; filter F_{A1}: ineffective
C	deposition: forced laminar flow; filter F_{A1}: same efficiency as filter F_{A3}
	Scott Gallery
A	deposition: forced laminar flow
B	deposition: homogeneous turbulence in the core of the room
	Sepulveda House
A	deposition: natural convection flow (0000–1000 and 1500–2400 h), homogeneous turbulence in the core of the room (1000–1500 h)

For the model calculations, each site was represented as a single well-mixed chamber, with building size and ventilation characteristics as indicated in Figure 1 and Table I. A constant ventilation rate was adopted for the Norton Simon Museum, based on the apparent dominance of the constantly operated mechanical ventilation system over infiltration. Likewise, the rate of outdoor air exchange at the Scott Gallery was taken to be constant, based on the small variance in results from tracer gas decay measurements. At the Sepulveda House, tracer decay data were used to obtain hourly averaged air exchange rates, which were then applied in the model calculations.

Particle removal efficiencies for filters F_{A3} and F_{B1} were based on measurements reported in Figure 2 for particles in the diameter range 0.09–2.3 μm. The efficiencies for particles smaller than 0.09 μm and larger than 2.3 μm in diameter were estimated to be the same as the measured efficiencies for the 0.09–0.13 and 1.7–2.3-μm sections, respectively. The charcoal filters, F_{A2} and F_{B2}, were assumed to have no effect on particle concentrations, on the basis of measurements of the penetration efficiency for F_{A2}. To best reflect the prevailing conditions on the monitoring day for this study, the effectiveness in removing particles of the newly replaced filter F_{A1} was taken to be zero, based on measurements showing its effectiveness to be less than 5% at that time. An additional modeling run (case C, see Table II) was carried out with filter F_{A1} having the same effectiveness as filter F_{A3}. The latter case better represents ordinary conditions at the Norton Simon Museum. [The particle filter material is contained in large rolls. Routinely, the filters are advanced a small fraction (<10%) of their exposed length, thereby maintaining a fairly uniform degree of particle loading. Just prior to the day of monitoring in this study, a new roll of material was installed for filter F_{A1}.]

Aerosol deposition rates were computed for idealized flow conditions by using the data on wall–air temperature differences and near-wall air velocities reproduced in Figure 3. These data were used to determine the hourly average temperature difference between the wall and the air. The temperature differences were than assumed to apply to all surfaces of the building. For the Sepulveda House, particle deposition was computed by using the natural convection description of air flow during 0000–1000 and 1500–2400 PST (*20*). Homogeneous turbulence in the

Table III. Average Mass Concentration ($\mu g\ m^{-3}$) of Aerosol Components for Study Periods from Filter-Based Measurements and Simulations

	fine			coarse[b]		
	EC[a]	soil dust	total	EC	soil dust	total
			Norton Simon Museum			
outdoor, measured	3.9	1.5	50	2.7	30	81
indoor, measured	0.67	0.15	9.3	0.09	0.25	−2.0
indoor, modeled, case A	0.83	0.36	12.5	0.10	1.0	2.9
indoor, modeled, case B	0.82	0.36	12.4	0.10	1.0	2.9
indoor, modeled, case C	0.62	0.30	10.1	0.004	0.04	0.11
			Scott Gallery			
outdoor, measured	1.5	0.75	26	0.95	6.9	37
indoor, measured	0.16	0.09	4.1	0.01	0.13	2.3
indoor, modeled, case A	0.23	0.08	3.7	0.05	0.32	1.8
indoor, modeled, case B	0.22	0.08	3.6	0.05	0.32	1.8
			Sepulveda House			
outdoor, measured	5.0	2.6	34	1.3	41	117
indoor, measured	5.6	0.86	24	0.75	23	57
indoor, modeled, case A	4.9	2.5	22	0.49	14	40

[a] Elemental carbon particles. [b] Coarse component data are obtained by difference between mass concentration determined for filters in open-faced holders and filters downstream of cyclones with ~2.0-μm-diameter cutpoint. The negative measured value at the Norton Simon Museum results from subtraction of two small and nearly identical measurement results.

core of the building was assumed to dominate deposition processes for the remaining period at this site. At the Norton Simon Museum and at the Scott Gallery, deposition calculations were carried out for two representations of near-wall air flows. As shown in Table II, the base case (case A) calculations were made assuming laminar, forced flow, parallel to the surfaces. Case B calculations were made assuming that the near-wall flows were dominated by homogeneous turbulence in the core of the rooms. A comparison of model and measurement results for particle deposition velocity at these two sites suggests that the actual deposition rates lie between the values predicted for case A and case B conditions at the Scott Gallery and closer to the results for case A relative to case B conditions at the Norton Simon Museum (*8*).

For deposition calculations based on laminar, forced flow, the free-stream air velocity, U_∞, is required to compute the deposition velocity. For laminar flow conditions, the air velocity probes located at ~0.6 and ~1.2 cm from the wall would be within the momentum boundary layer. The hourly averaged free-stream air velocity was estimated from velocity measurements with these probes using the boundary layer velocity profile for an isolated flat plate (*25*). This free-stream velocity was assumed to apply for all indoor surfaces. The mean hourly averaged value [± one standard deviation (SD)] of the free-stream air velocity so obtained was 0.33 ± 0.11 m s^{-1} for the Norton Simon Museum and 0.29 ± 0.04 m s^{-1} for the Scott Gallery.

For calculations based on the assumption of homogeneous turbulence, the turbulence intensity parameter, K_e, was estimated on an hourly basis from the air velocity, linearly interpolated to a distance of 1 cm from the wall, by use of the relationship proposed by Corner and Pendlebury (*26*):

$$K_e = k_o^2 \frac{0.073}{\mu} \frac{\rho u^2}{2} \left(\frac{\mu}{\rho u X} \right)^{1/5} \qquad (2)$$

where k_o is von Kármán's constant, taken to be 0.4, μ is the dynamic viscosity of air, ρ is the air density, u is the mean air velocity, and X is the length of the surface in the direction of the mean motion. This equation is based on a correlation for the turbulent drag on a flat plate in an infinite fluid moving parallel to the plate. The turbulence intensity parameter so obtained has a mean hourly averaged value (±1 SD) of 0.56 ± 0.34 s^{-1} for the Norton Simon Museum, 1.25 ± 0.45 s^{-1} for the Scott Gallery, and 0.18 ± 0.04 s^{-1} for the period 1000–1500 PST at Sepulveda House. Note that the results of other studies of pollutant deposition velocity based on measurements inside buildings are bounded approximately by predictions based on the assumption of homogenous turbulence with K_e in the range 0.1–10 s^{-1} (*20*).

For each site, a comparison is presented in Figure 4 of the results of outdoor measurements, indoor measurements, and the indoor model predictions (under case A conditions) for the total fine particle concentration as a function of time and for the 24-h-average aerosol size distribution. At both the Norton Simon Museum and the Scott Gallery, the fine particle mass concentration indoors is reduced to 15–20% of the outdoor value and coarse aerosol mass present indoors is less than 5% of the outdoor value. The agreement between the indoor model and measurement results ranges from excellent to good: the size distribution and total fine aerosol concentration is predicted quite accurately for the Scott Gallery, while at the Norton Simon Museum the agreement is good except that the aerosol mass concentration for particles having a diameter in the range 0.18–0.35 μm is overpredicted by the indoor air quality model.

At the Sepulveda House, there is little difference between the indoor and outdoor fine particle concentrations. The model reflects this fact; however, the high-frequency fluctuations in the indoor concentration, which result from the high air-exchange rate, are smoothed in the model calculations, an artifact of using hourly averages for outdoor concentrations in the model. (Although the model as used here employs outdoor aerosol concentration data on an hourly averaged basis, there is no intrinsic reason in the method of solution that precludes using data with finer time resolution.) One does not need a detailed mathematical model to predict the indoor concentrations of fine particles based on outdoor values if the building has a high air-exchange rate and no filtration. However, the estimates of particle flux to the walls and other surfaces of the Sepulveda House are complex and utilize the indoor air quality model's capabilities.

Table III compares measurements and predictions of the aerosol constituents, sorted according to particle size into coarse and fine modes. Again, the agreement is good,

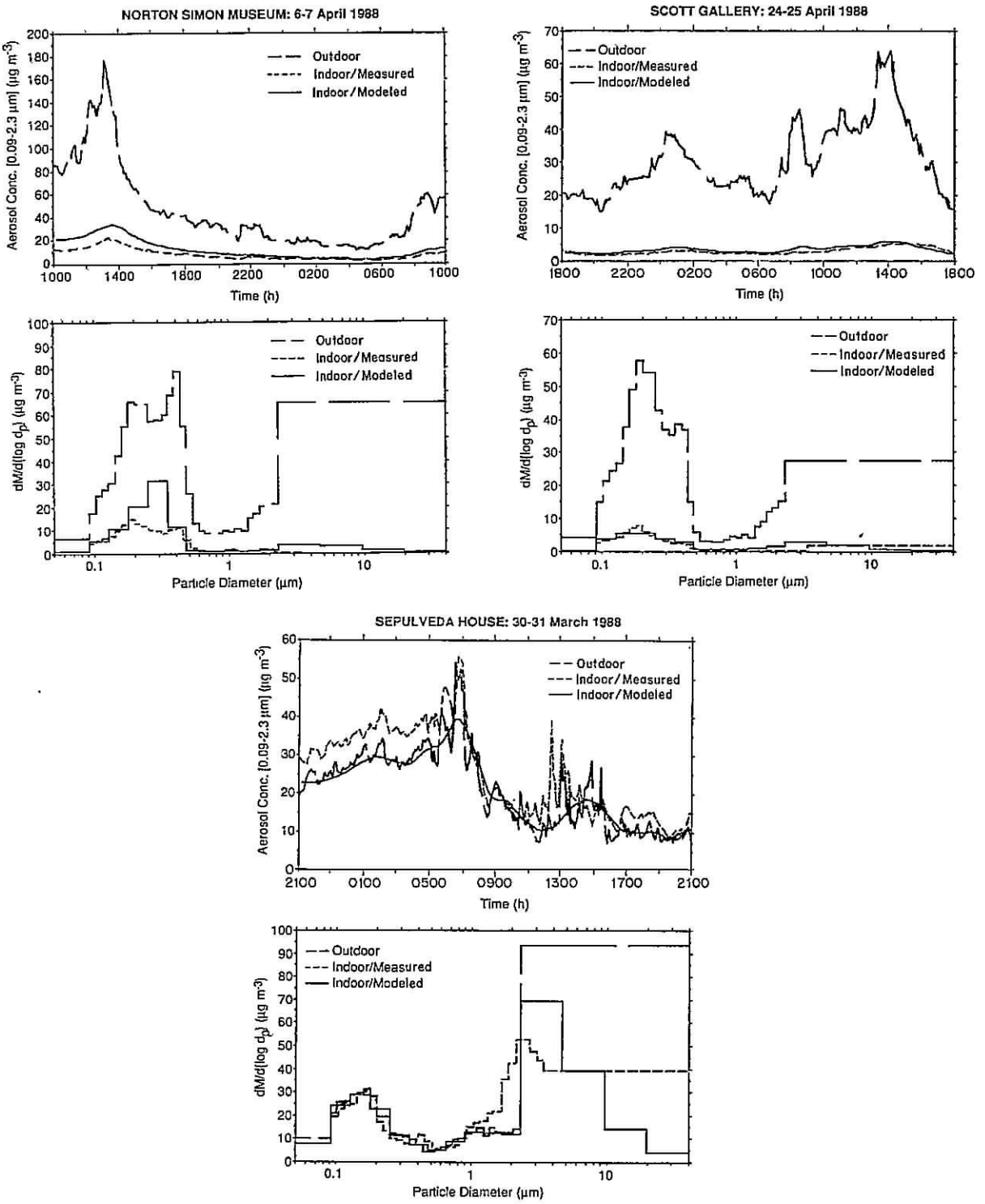

Figure 4. Fine aerosol mass concentration vs time and 24-h-average aerosol size distribution for the three study sites. The figure compares outdoor measurements, indoor measurements, and indoor modeling results. The measured fine particle concentrations are based on the midrange optical particle counters. The coarse component, and the mass in the smallest section of the size distribution, are based on analysis of filter samples. The modeling results for the Norton Simon Museum and the Scott Gallery reflect case A conditions defined in Table II.

particularly for the fine particles for which the input data are more detailed.

Overall, the agreement between model calculations and measurement results justifies confidence in using the model to further consider the dynamics of indoor aerosols. The next two sections explore the fate of particles and the magnitude of the soiling hazard in museums.

Fate of the Particles Entering from Outdoor Air

The design of effective control measures for indoor aerosols can be facilitated by examining the relative strengths of particle sources and sinks. For the three sites considered in this paper, the overwhelming source of indoor airborne particles during these experiments was due to the entry of outdoor air. The validity of this observation is substantiated by the agreement between measurement and model results. It remains to consider the relative strength of the aerosol sinks: filtration, removal by ventilation, and deposition onto interior surfaces. Coagulation, which serves as a sink for very fine particles, transferring their mass to larger particles, is also considered.

For each simulation and for each particle size section,

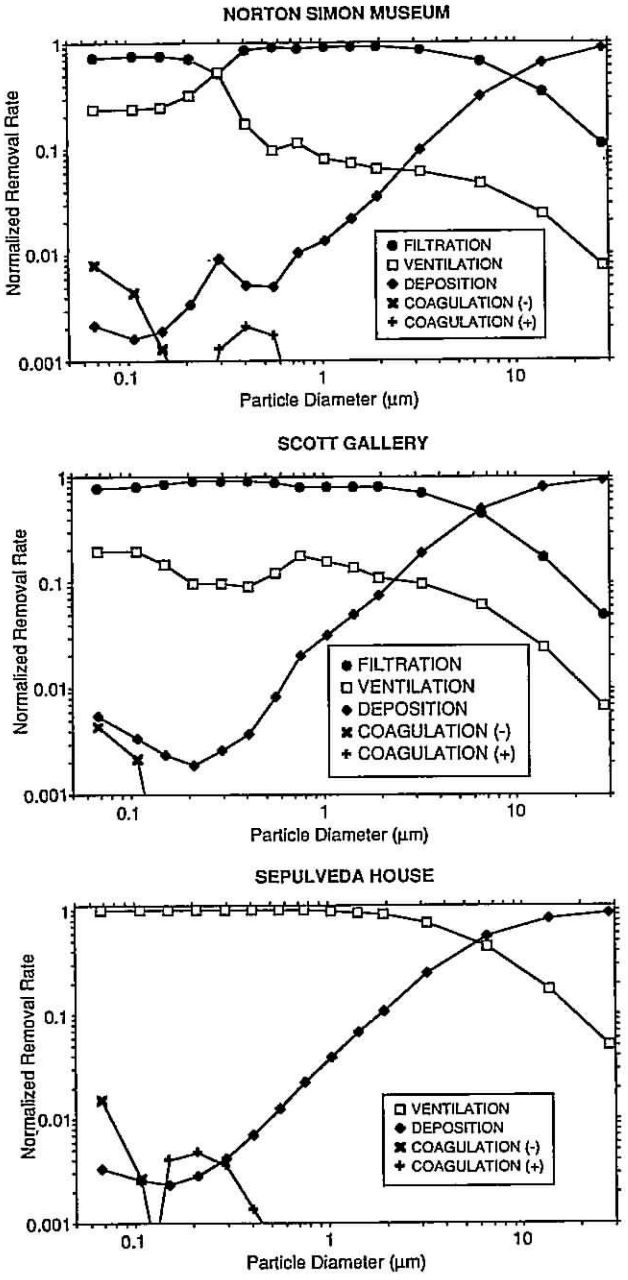

Figure 5. Predicted fate of particles introduced into the buildings from outdoors. The ordinate of each point represents the 24-h-average fraction of the mass in that section brought in from outdoors that is removed by the indicated process. The abscissa reflects the logarithmic midpoint of the range of diameters in the size section. Coagulation (–) indicates a net loss of aerosol mass in the section due to particle coagulation, and Coagulation (+) indicates a net gain. The results shown for the Norton Simon Museum and the Scott Gallery reflect the case A conditions defined in Table II.

the mean rate of removal of aerosol mass by the various sinks was computed and then normalized in each case by the mean rate of supply of aerosol mass in the section from outdoor air. The results for case A, displayed in Figure 5, show that at the Norton Simon Museum and at the Scott Gallery the dominant fate of particles smaller than approximately 10 μm in diameter is removal by the filters. This result is obtained despite the moderately low particle filtration efficiencies, because during its residence time within these museums, air makes a large number of passes through the filters in the recirculating air ducts. At Sepulveda House, particles of this size are predominantly removed by ventilation. Surprisingly, at all three sites the dominant fate of larger particles is deposition onto surfaces, essentially entirely by gravitational settling onto the floor and other upward-facing surfaces. This result demonstrates the importance of an effective filter for removing coarse particles from the inlet outdoor air. Under ordinary conditions at the Norton Simon Museum, with filter F_{A1} partially loaded with particles rather than clean, it is expected that 95% or more of coarse particles are removed from the air entering the building.

Deposition constitutes a much smaller sink for fine particles; for example, for particles that are 0.1 μm in diameter, only 0.1–0.5% of those that enter the buildings will ultimately deposit on a surface. This result indicates that detailed calculations of deposition rates are not necessary to obtain accurate predictions of the indoor airborne concentrations of fine particles in these particular buildings.

At all three sites, and for all particle sizes, coagulation is seen to be of little importance. It is not correct to conclude, however, that particle coagulation is never important in indoor air. Conditions at these three sites tend to minimize the rates of coagulation: low particle concentrations at the Norton Simon Museum and at the Scott Gallery imply low particle collision rates, and the high air-exchange rate at Sepulveda House does not allow sufficient time for coagulation to have a significant effect. On the other hand, previous analysis of the fate of cigarette smoke in a room having a low air-exchange rate showed that coagulation was an important sink for particles smaller than 0.2 μm in diameter (*4*).

Particle Deposition onto Indoor Surfaces

Even though only a small fraction of the fine particles that enter a building deposit onto surfaces, the soiling hazard posed by particle deposition may still be significant. To assess the magnitude of the problem, the rates of particle accumulation onto the floor, walls, and ceiling of each of the three sites were computed by using the indoor air quality model for the 24-h study periods. The results are displayed in Figure 6 in terms of the rate of mass accumulation per unit surface area, J, as a function of particle size and composition. Table IV gives the total rate of accumulation of elemental carbon, soil dust, and the total aerosol onto the walls, floors, and ceilings for each of the three sites. Before considering the significance of the results, it is important to emphasize that the calculations at each site represent predictions for a single day. Thus, extrapolations to longer time periods must be regarded only as indicative estimates. In particular, differences in the deposition rates between sites may reflect differences in the outdoor conditions on the particular days studied, rather than differences in the long-term average rates of soiling. Note, also, that although the calculations are done specifically for the floor, walls, and ceiling, the results are indicative of expected values for other surfaces, such as those of art objects, that have corresponding orientations. Finally, there is preliminary evidence suggesting that particles larger than a few micrometers in diameter deposit onto vertical surfaces at rates that are substantially larger than predicted by the deposition mechanisms included in the indoor air quality model. Thus, deposition rates of aerosol mass to the walls and ceiling probably represent lower bounds, particularly for the soil dust component, which is found primarily in the coarse particle mode.

Given these cautions, the computed total rate of accumulation of elemental carbon particles onto the walls of the three sites is in the range of 0.02–0.7 $\mu g\ m^{-2}\ day^{-1}$. The corresponding rates for the ceilings are smaller, 0.002–0.5 $\mu g\ m^{-2}\ day^{-1}$, and are very sensitive to the assumed nature

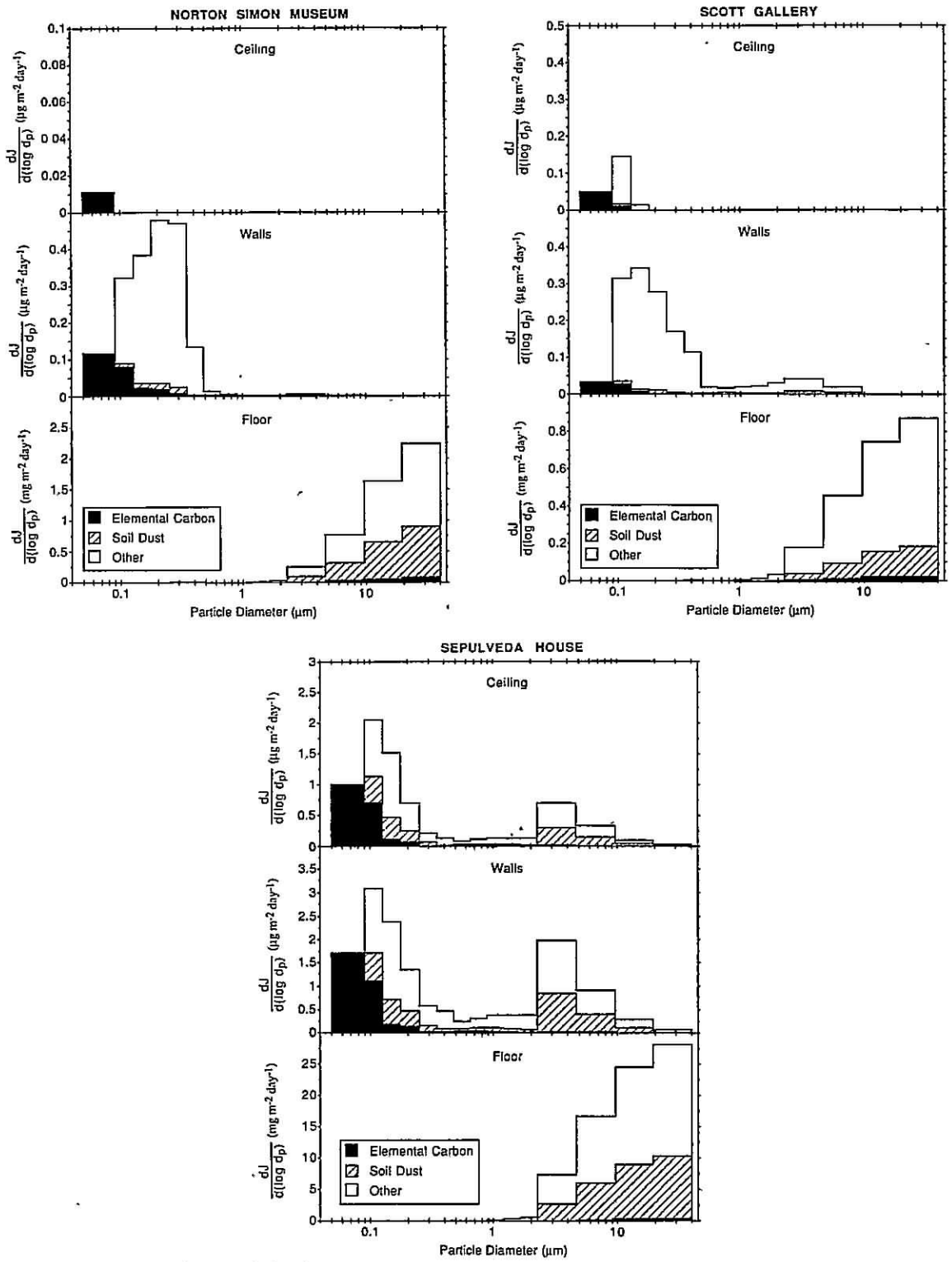

Figure 6. Predicted average rate of accumulation, based on the single study day, of aerosol mass as a function of particle composition and size for three major surface orientations. Note that the vertical axes have different scales; in particular, the mass unit for the floors is milligram, compared with microgram for the other surfaces. The results shown for the Norton Simon Museum and the Scott Gallery reflect the case A conditions defined in Table II.

of near-surface air flow. For forced laminar flow conditions (case A), gravitational settling is effective in reducing deposition of ~0.1-μm particles onto the ceiling. For homogeneous turbulence (case B), however, eddy diffusivity dominates gravitational settling for the very fine elemental carbon particles, and the deposition rate is about the same for the ceiling as for the walls. The rates of accumulation of elemental carbon onto the floors are much larger, 2–50 $\mu g\ m^{-2}\ day^{-1}$ for the Norton Simon Museum, 20 $\mu g\ m^{-2}\ day^{-1}$ for the Scott Gallery, and almost 300 $\mu g\ m^{-2}\ day^{-1}$ for Sepulveda House. The particle sizes associated with volume-weighted elemental carbon deposition onto these surfaces are quite distinct: predominantly 0.05–0.3 μm for the walls and ceiling, compared with 4–40 μm for the floor. However, considered in terms of the rate of accumulation of projected particle cross-sectional area [probably the appropriate scale for assessing the rate of soiling (27)], the deposition of fine particles onto the floor has a significance comparable with the deposition of coarse particles.

Table IV. Average Deposition Rate of Aerosol Mass ($\mu g\ m^{-2}\ day^{-1}$) onto Indoor Surfaces Based on Simulations of Study Periods at Each Site

	EC[a]	soil dust[b]	total
	Norton Simon Museum—Case A		
ceiling	0.003	(0.000)	0.003
walls	0.050	(0.010)	0.30
floor	52	560	1540
	Norton Simon Museum—Case B		
ceiling	0.54	(0.10)	3.6
walls	0.64	(0.23)	6.2
floor	53	560	1540
	Norton Simon Museum—Case C		
ceiling	0.002	(0.000)	0.002
walls	0.039	(0.007)	0.24
floor	2.4	23	67
	Scott Gallery—Case A		
ceiling	0.015	(0.001)	0.036
walls	0.017	(0.008)	0.22
floor	19	130	710
	Scott Gallery—Case B		
ceiling	0.26	(0.08)	3.0
walls	0.29	(0.13)	3.9
floor	19	130	710
	Sepulveda House—Case A		
ceiling	0.40	(0.32)	1.4
walls	0.69	(0.70)	2.8
floor	280	8500	24,000

[a] Elemental carbon particles. [b] The soil dust results for walls and ceilings represent lower bounds. Inertial effects, which may be important for coarse particle deposition to these surfaces, are not included in the model predictions of deposition.

Because of its lower rate of accumulation, soil dust appears to pose a smaller soiling hazard than elemental carbon for the ceiling and walls at the Norton Simon Museum and at the Scott Gallery. However, the rates of accumulation of soil dust onto the floor at those two sites are 7–10 times larger than those of soot. These differences are a consequence of the fact that soil dust, being mechanically generated, is found predominantly in the coarse particle mode and settles onto upward facing surfaces under the influence of gravity, whereas elemental carbon, produced in combustion systems, is found primarily in fine particles for which deposition occurs to surfaces of any orientation by a combination of advective diffusion and thermophoresis (*20*).

The much higher flux density of particle mass to the floor compared with values for the ceiling and walls points to another limitation of the calculations employed here in assessing the soiling hazard for certain surfaces. In these calculations, vertical surfaces are assumed to be smooth; however, many real surfaces are rough. Through gravitational settling, large particles will deposit preferentially on the upward-facing portions of surface roughness elements. Because contrast is readily detected, nonuniform deposition of elemental carbon particles by such a process would probably lead to noticeable visual degradation of the object more rapidly than an equivalent rate of deposition spread uniformly over the surface.

To gain perspective on the significance of these results in the context of protecting museum collections, a characteristic time interval for soiling was computed. Previous studies have shown that a white surface is perceptibly darkened when 0.2% of its area is effectively covered either by black dots that are too small to be distinguished individually (*27*) or by black particles (*28*). Since the light-absorbing properties of elemental carbon particles

Table V. Characteristic Time (Years) for Perceptible Soiling to Occur[a,b]

	ceiling		walls		floor	
case	$\tau_{s;EC}$	$\tau_{s;SD}$	$\tau_{s;EC}$	$\tau_{s;SD}$	$\tau_{s;EC}$	$\tau_{s;SD}$
	Norton Simon Museum					
A	180		12	(170)	1.2	0.2
B	1.2	(12)	1.1	(8.4)	0.6	0.2
C	230		16	(210)	4.7	3.0
	Scott Gallery					
A	35	(720)	40	(240)	2.9	0.6
B	2.5	(19)	2.4	(16)	1.4	0.6
	Sepulveda House					
A	1.5	(6.2)	0.9	(4.1)	0.15	0.01

[a] Based on the predicted deposition rates for the single study day at each site. The characteristic soiling time is computed as the time required for the accumulation of sufficient elemental carbon particles ($\tau_{s;EC}$) or soil dust particles ($\tau_{s;SD}$) onto a smooth surface to effectively cover 0.2% of the surface area. For black particles on a white surface, this degree of coverage has been shown to yield perceptible soiling (*27*, *28*). [b] Predictions of particle deposition rate do not include inertial effects, which may be important for coarse particle sizes, where most of the soil dust is found. Therefore, the characteristic times for perceptible soiling to occur on walls and ceilings due to soil dust deposition represent upper limits. For floors, deposition of coarse particles is dominated by gravitational settling, and so the estimates are believed to be accurate.

differ from those of soil dust, the degree of surface coverage needed to produce perceptible soiling probably differs for the two components. The information needed to combine the accumulation rate of the two components into a single soiling rate is lacking, and so, for the present study, the characteristic times for soiling by elemental carbon particles ($\tau_{s;EC}$) and by soil dust ($\tau_{s;SD}$) were estimated as the time required to achieve 0.2% coverage of a surface by these components independently. These times were computed for each surface orientation and each model case, given the deposition rates as a function of size (as displayed for case A in Figure 6), and assuming that, within each section, the deposited elemental carbon or soil dust can be considered to exist as pure, spherical particles with a diameter equal to the logarithmic mean for the section. Then, the characteristic time for a perceptible deposit of either component to accumulate is given by

$$\tau_{s;c} = 0.002\left[\sum_i \left(\frac{3}{2d_i}\right)\left(\frac{\Delta J_{i;c}}{\rho}\right)\right]^{-1} \qquad (3)$$

where c represents the soiling component (EC or SD), d_i is the particle diameter for section i, $\Delta J_{i;c}$ is the rate of mass deposition of component c for section i, and ρ is the particle density.

The resulting values for $\tau_{s;c}$ are given in Table V for the three sites. For walls and ceilings, deposition of elemental carbon particles appears to constitute a greater soiling hazard than the deposition of soil dust. Characteristic soiling times associated with elemental carbon particle deposition are in the range 1–40 years for walls. For ceilings, the corresponding predictions are in the range 1–35 years except for the Norton Simon Museum under the assumption of forced laminar flow for which the estimated characteristic soiling time is 2 centuries. For floors, predicted characteristic soiling times due to soil dust deposition are shorter than those due to elemental carbon deposition. The values of $\tau_{s;SD}$ range from as short as 3 days at the Sepulveda House to as long as 3 years for the Norton Simon Museum with an effective intake filter (case C). Among the three surface orientations, predictions for the ceilings must be regarded as the least certain, since,

as with the walls, the deposition rates depend critically on near-surface air flows, and no measurements of flows near ceilings were made in this study.

With the exception of the few large values of τ_s for the ceiling of the Norton Simon Museum, these soiling periods are short relative to the time scales over which museum curators wish to preserve their collections. In some respects, however, these estimates are conservative. For example, the degree of effective area coverage by black particles needed to produce perceptible soiling would be a minimum for a purely white surface for which the 0.2% result applies. The surfaces of heavily pigmented paintings could probably accrue a greater deposit before soiling became perceptible.

As expected, the soiling problem is most acute at the Sepulveda House because of its high ventilation rate and lack of particle filtration. Taking the geometric mean of the results for cases A and B as an estimate of the true soiling rates at the Norton Simon Museum and the Scott Gallery, soiling rates due to elemental carbon deposition at these sites are approximately 5–10 times lower than at the Sepulveda House. For soil dust deposition onto upward surfaces, the difference between the characteristic soiling time at the Sepulveda House and those at the other two sites is even greater. It is noteworthy that the effectiveness of the supply air filter at the Norton Simon Museum in lengthening the soiling periods (compare cases A and C) is not large for soiling by elemental carbon particles. This result is obtained because the deposition of fine particles onto the floor contributes significantly to $\tau_{s;EC}$, and the inlet filter is relatively ineffective in removing these particles. On the other hand, an effective supply air filter at the Norton Simon Museum does significantly extend the characteristic soiling time for the floor associated with soil dust deposition.

Discussion

The results of this study serve several purposes. First, they substantially increase the basis for confidence in the ability to predict the size distribution and chemical composition of the indoor aerosol by use of the indoor air quality model previously described (*4*). Second, they provide considerable information beyond that previously available about the indoor–outdoor aerosol relationship for two types of buildings. (The Norton Simon Museum and the Scott Gallery are representative of modern commercial buildings, apart from their relatively high ratio of recirculated air to outdoor make-up air flow rates and the presence of activated carbon filters. Sepulveda House is representative of many older buildings, at least those in temperate climates.) Third, the results constitute, to our knowledge, the first detailed estimates of the cause-and-effect relationships that lead to soiling of indoor surfaces. The information about the size of particles that contribute to soiling is crucial in designing efficient control measures. Estimates of the rate of soiling will help concerned officials make informed decisions about how much of their limited resources to devote to control measures.

In addition to the progress marked by the results reported here, related papers address associated issues: a direct and sensitive test of the deposition calculations (*8*), and an evaluation of options available for controlling the soiling of indoor surfaces (*29*). Because of the nature of the experiments reported here, particle generation due to occupant activities and other indoor sources, to the extent that it occurs, will be underrepresented. Data from long-term studies suggest that the provision of outdoor air for ventilation is the largest source of airborne particles in five southern California museums—including the three considered here (*5*). Nevertheless, to protect works of art from soiling, it is important to limit indoor aerosol sources (*29*).

The other hazard for artwork associated with the deposition of particles—corrosion and other chemical attack—has not been addressed specifically here. The potential for chemical damage caused to the surfaces of art objects from particle deposition should be investigated.

In addition to these topics, there is a need for further investigation of the relationship between the deposition rate of elemental carbon and other particles and the rate of optical degradation of surfaces. Results of such studies are needed to refine estimates of the time periods over which perceptible soiling occurs.

With the capability of testing candidate protection measures and ventilation system designs in advance of their construction by using a model such as the one employed here, the ability to protect artwork from soiling due to the deposition of airborne particles will improve. It may become not only possible but practical to greatly increase the time periods over which artwork can be preserved while retaining the visual qualities given by the artist.

Acknowledgments

We thank Robert Harley, Michael Jones, and Wolfgang Rogge for assisting with the field experiments; Timothy Ma for fabricating the thermistor array and signal conditioning electronics; Luiz Palma for assisting with the performance evaluation of the optical particle counters; Richard Sextro for arranging a loan of a portable gas chromatograph; and the staffs of the three museum sites for their generous cooperation. The X-ray fluorescence analyses were carried out by Dr. John Cooper at NEA, Inc. Robert Cary at Sunset Laboratories measured the elemental carbon content of filter samples.

Registry No. Carbon, 7440-44-0.

Literature Cited

(1) Thomson, G. *The Museum Environment*; Butterworths: London, 1978.
(2) Yocum, J. E. *J. Air Pollut. Control Assoc.* **1982**, *32*, 500–520.
(3) Baer, N. S.; Banks, P. N. *Int. J. Museum Manage. Curatorship* **1985**, *4*, 9–20.
(4) Nazaroff, W. W.; Cass, G. R. *Environ. Sci. Technol.* **1989**, *23*, 157–166.
(5) Ligocki, M. P.; Salmon, L. G.; Fall, T.; Jones, M. C.; Nazaroff, W. W.; Cass, G. R. Characteristics of airborne particles inside Southern California museums. California Institute of Technology, Pasadena (manuscript in preparation).
(6) Nazaroff, W. W.; Cass, G. R. *Environ. Sci. Technol.* **1986**, *20*, 924–934.
(7) Ligocki, M. P.; Liu, H. I. H.; Cass, G. R.; John, W. Measurements of particle deposition rates inside Southern California museums, submitted for publication in *Aerosol Sci. Technol.*
(8) Nazaroff, W. W.; Ligocki, M. P.; Ma, T.; Cass, G. R. Particle deposition in museums: Comparison of modeling and measurement results, submitted for publication in *Aerosol Sci. Technol.*
(9) Nazaroff, W. W. Ph.D. Thesis, California Institute of Technology, Pasadena, CA, 1989; pp 200–206.
(10) Gray, H. A.; Cass, G. R.; Huntzicker, J. J.; Heyerdahl, E. K.; Rau, J. A. *Environ. Sci. Technol.* **1986**, *20*, 580–589.
(11) John, W.; Reischl, G. *J. Air Pollut. Control Assoc.* **1980**, *30*, 872–876.
(12) Johnson, R. L.; Shah, J. J.; Cary, R. A.; Huntzicker, J. J. In *Atmospheric Aerosol: Source/Air Quality Relationships*; Macias, E. S., Hopke, P. K., Eds.; ACS Symposium Series 167; American Chemical Society: Washington, DC, 1980; pp 223–233.

(13) Cary, R. Presented at the Third International Conference on Carbonaceous Particles in the Atmosphere, Berkeley, CA, October 1987.
(14) Dzubay, T. G. *X-ray Fluorescence Analysis of Environmental Samples*; Ann Arbor Science: Ann Arbor, MI, 1977.
(15) Mulik, J.; Puckett, R.; Williams, D.; Sawicki, E. *Anal. Lett.* **1976**, *9*, 653–663.
(16) Bolleter, W. T.; Bushman, C. T.; Tidwell, P. W. *Anal. Chem.* **1961**, *33*, 592–594.
(17) Cass, G. R.; Conklin, M. H.; Shah, J. J.; Huntzicker, J. J.; Macias, E. S. *Atmos. Environ.* **1984**, *18*, 153–162.
(18) *ASHRAE Handbook: 1985 Fundamentals*; American Society of Heating, Refrigerating, and Air Conditioning Engineers: Atlanta, GA, 1985; Chapter 22.
(19) Nazaroff, W. W.; Cass, G. R. *J. Aerosol Sci.* **1987**, *18*, 445–454.
(20) Nazaroff, W. W.; Cass, G. R. Mass-transport aspects of pollutant removal at indoor surfaces. *Environ. Int.*, in press.
(21) Schiller, G. E. Ph.D. Thesis, University of California, Berkeley, CA, 1984.
(22) Bejan, A. *Convection Heat Transfer*; Wiley: New York, 1984.
(23) Ouimette, J. Ph.D. Thesis, California Institute of Technology, Pasadena, CA, 1981.
(24) Miller, M. S.; Friedlander, S. K.; Hidy, G. M. *J. Colloid Interface Sci.* **1972**, *39*, 165–176.
(25) Schlichting, H. *Boundary-Layer Theory*, 7th ed.; McGraw-Hill: New York, 1979; pp 315–321.
(26) Corner, J.; Pendlebury, E. D. *Proc. Phys. Soc., London* **1951**, *B64*, 645–654.
(27) Carey, W. F. *Int. J. Air Pollut.* **1959**, *2*, 1–26.
(28) Hancock, R. P.; Esmen, N. A.; Furber, C. P. *J. Air Pollut. Control Assoc.* **1976**, *26*, 54–57.
(29) Nazaroff, W. W.; Cass, G. R. Protecting museum collections from soiling due to the deposition of airborne particles. California Institute of Technology, Pasadena. Manuscript in preparation.

Received for review January 9, 1989. Accepted July 31, 1989. This work was supported by a contract with the Getty Conservation Institute and by fellowships from the Switzer Foundation and the Air Pollution Control Association (subsequently renamed Air and Waste Management Association).